

## Experimental Study of Poloidal Flow Effect on Magnetic Island Dynamics in LHD and TJ-II

Y. Narushima 1), F. Castejón 2), S. Sakakibara 1), K. Y. Watanabe 1), S. Ohdachi 1), Y. Suzuki 1), T. Estrada 2), F. Medina 2), D. López-Bruna 2), M. Yokoyama 1), M. Yoshinuma 1), K. Ida 1), LHD Experiment Group 1) and TJ-II Experiment Group 2)

1) National Institute for Fusion Science, 322-6 Oroshi-cho, Toki 509-5292, Japan

2) Laboratorio Nacional de Fusión. CIEMAT. Avenida Complutense 22, 28040 Madrid, Spain

E-mail contact of main author: narusima@LHD.nifs.ac.jp

**Abstract.** The dynamics of a magnetic island are studied by focusing on the poloidal flows in the helical devices LHD and TJ-II. The temporal increment of the  $\mathbf{E} \times \mathbf{B}$  poloidal flow prior to the magnetic island transition from growth to healing is observed. The direction of the poloidal flow is in the electron-diamagnetic direction in LHD and in the ion-diamagnetic direction in TJ-II. From the magnetic diagnostics, it is observed that a current structure flowing in the plasma moves  $\sim \pi$  rad poloidally in the electron-diamagnetic direction during the transition in LHD experiments. These experimental observations from LHD and TJ-II show that the temporal increment of the poloidal flow is followed by the transition (growth to healing) of the magnetic island regardless of the flow direction and clarify the fact that significant poloidal flow affects the magnetic island dynamics.

### 1. Introduction

Nested flux surfaces are generally required for good plasma confinement in toroidal plasmas. Magnetic islands have a strong influence on transport and, moreover, in the tokamak case, they can give rise to multiple catastrophic phenomena like NTMs and interchange modes [1], while in stellarators islands are basic for divertor configurations [2] as well as for creating transport barriers [3]. An important difference between tokamaks and stellarators regarding island behaviour is that the sign of the magnetic shear is opposite in these devices, which causes the dynamics to be notably different. Some reports [4,5] about heliotron plasmas suggest that the magnetic island might play a key role to improve the confinement and/or MHD stabilities. Furthermore, it has been reported that the confinement is not degraded seriously as long as the magnetic island does not grow under a certain finite magnetic shear configuration [6,7]. And also, it has been reported that the magnetic island is able to trigger Core Electron Root Confinement (CERC) in TJ-II [8]. It is thought that the production and control of optimised magnetic islands enable us to obtain high-performance plasmas. Therefore, the study of the dynamics of magnetic islands is a critical issue. This paper is organized as follows. The experimental set-up and results in LHD are described in the following section. In Section 3, the experimental set-up and experimental results in TJ-II are shown. We discuss the results in Section 4 and, finally, summarize in Section 5.

### 2. Experiments in LHD

#### 2.1. Experimental Setup of LHD

The Large Helical Device (LHD) [9] is the largest Heliotron-type plasma confinement device with poloidal/toroidal period numbers of 2/10, equipped with superconducting helical and poloidal coils. Typical plasma major and averaged minor radii are  $R = 3.6$  and  $a = 0.6$  m, respectively. The typical rotational transform ( $\iota/2\pi$ ) profile has minimum  $\iota/2\pi = 0.3$  at the magnetic axis and a maximum  $\iota/2\pi = 1.6$  at the edge. The position of the  $\iota/2\pi = 1$  surface is at

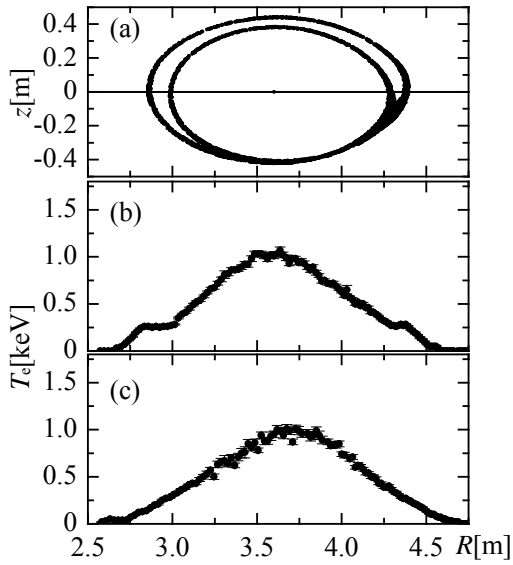


Fig.1 (LHD) (a) Poincaré plot of magnetic island in vacuum configuration. Electron temperature profile with (b) grown island and (c) healed island.

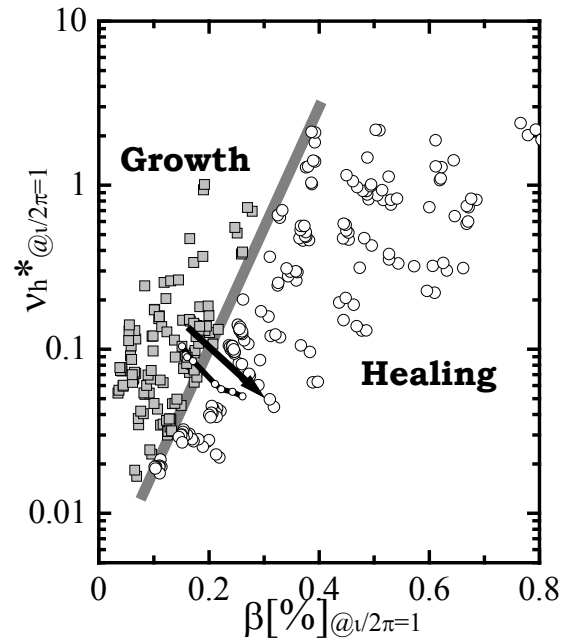


Fig.2 (LHD) Island growing (squares) and healing (circles) region in  $\beta$ - $\nu$  space. Boundary is drawn by grey solid line. Black solid line indicates trajectory of typical single discharge.

around  $\rho = 0.9$ . Here,  $\rho$  is the normalized minor radius. The magnetic island intended here has  $m/n = 1/1$  Fourier components (Here,  $m/n$  means poloidal/toroidal mode numbers), which can be made by the perturbation coils in the vacuum configuration as shown in Fig.1 (a).

Perturbation coils are placed on the top and bottom of LHD at intervals of  $0.2\pi$ [rad] in the toroidal circumference [10]. The Thomson scattering system measures the  $T_e$  profile. The measured points and the spatial resolution are 140 and 20–30 mm, respectively, and the typical sampling frequency is from 10 Hz to 80 Hz. The poloidal flow is diagnosed with charge-exchange spectroscopy (CXS) [11] with a time resolution of 0.1 s. The measured poloidal flow can be assumed as  $\mathbf{E} \times \mathbf{B}$  flow  $\omega_{E \times B}$ . Magnetic diagnostics can detect the perturbed magnetic field which appears when the magnetic island changes with time [12].

## 2.2. Characteristics of Magnetic Island in Quasi-Steady State

In the LHD experiments, the magnetic island grows or disappears during a discharge. When the magnetic island grows, the  $T_e$  profile shows significant local flattening as shown in Fig.1 (b), while the flattening disappears when the island is healed (Fig.1 (c)). The characteristics of the island dynamics in quasi-steady state were summarised in the parameter space of beta  $\beta$  and collisionality  $\nu$  as shown in Fig.2 [13]. The magnetic island grows in the lower- $\beta$  and higher- $\nu$  regime and disappears in the higher- $\beta$  and lower- $\nu$  regime. The boundary between growth and healing can be seen clearly, which is drawn by a grey solid line in Fig.2.

## 2.3. Experimental Results in Transient State (growth to healing)

To clarify the dynamic behaviour of the magnetic island intersecting the boundary between growth and healing, the heating power of the neutral beam (NB) is controlled in a single

discharge. The black solid line intersecting the grey solid line in Fig.2 is a typical trajectory of such a plasma.

The profiles of  $T_e$  measured near the O-point of the island are shown by closed circles in Fig.3 (b-d). The resonant surface of  $\nu/2\pi = 1$  lies at  $r_{\text{eff}} = 0.55\text{m}$ . The local flattening of the  $T_e$  profile indicates the existence of the magnetic island at  $t = 2.333\text{s}$  and  $2.533\text{s}$  shown by the horizontal lines in Fig.3 (b)(c). After that, the island disappears at  $t = 2.933\text{s}$  (Fig.3 (d)). The profiles of poloidal flow ( $\omega_{E \times B}$ ) measured near the X-point of the island are also shown by open circles in Fig.3 (b-d). (It should be noted that the toroidal angle of the measurement position is different from that of  $T_e$ .) The positive (negative) value of  $\omega_{E \times B}$  indicates the ion (electron)-diamagnetic direction. During the magnetic island healing, the absolute value of the poloidal flow  $|\omega_{E \times B}|$  in the electron-diamagnetic direction lying at  $r_{\text{eff}} = 0.6\text{m}$  increases with time and its profile becomes wide.

The relationship between the poloidal flow and flattening width of  $T_e$  is shown in Fig.4, in which results from multiple shots are plotted and the temporal trend is shown by an arrow. It

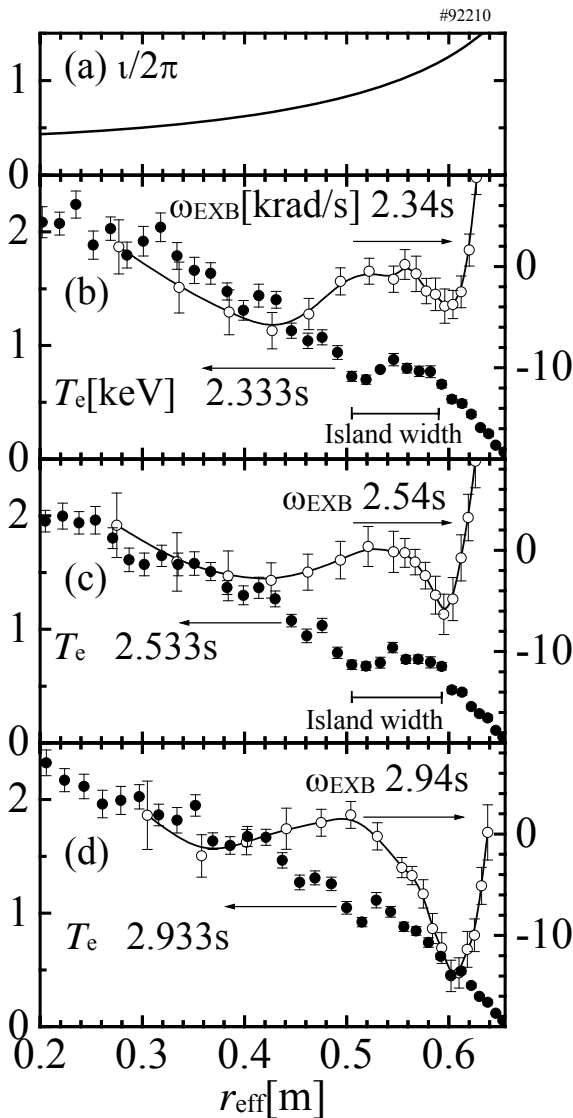


Fig.3 (LHD) Radial profile of (a)  $\nu/2\pi$ , (b-d)  $T_e$  (closed), and  $\omega_{E \times B}$  flow (open). The island (local flattening at  $r_{\text{eff}} \sim 0.55\text{m}$ ) transits from growth to healing. The  $|\omega_{E \times B}|$  at  $r_{\text{eff}} \sim 0.6\text{m}$  increases with time prior to the island being healed..

is clearly seen that the poloidal flow  $|\omega_{E \times B}|$  increases prior to the magnetic island healing. The flattening width of  $T_e$  is reduced in some cases below  $\omega_{E \times B} \sim -5\text{krad/s}$ , and there exists a threshold of  $\omega_{E \times B}$  between  $-5$  and  $-8\text{krad/s}$  for healing.

During the transition of magnetic island, the perturbed magnetic field  $\Delta\Phi^r$  profile shows an interesting behaviour. The perturbed magnetic field is detected when the island structure deviates from that of the seed island [10]. Figure 5 shows the poloidal profile of the perturbed magnetic field ( $\delta\Phi^r$ ) when the seed island grows (Fig.5 (a)) and disappears (Fig.5 (b)). The resonant field amplitude ( $\Delta\Phi^r_{m=1}$ ) is defined as the

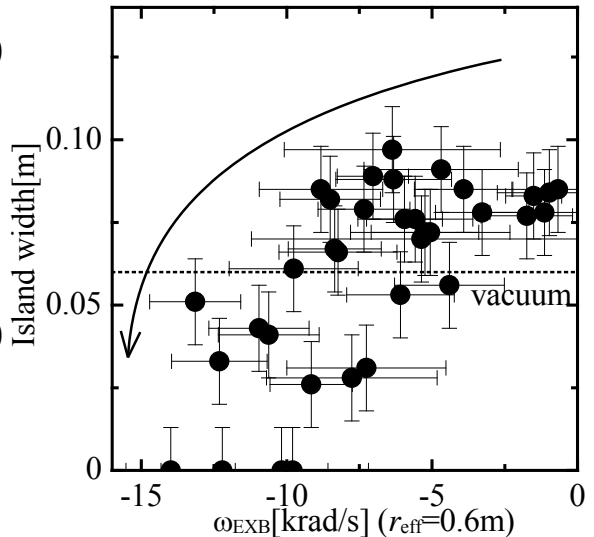


Fig.4 (LHD) Relationship between  $\omega_{E \times B}$  and island width. Dashed line indicates vacuum island width. Solid arrow shows time trend. Island width decreases when  $\omega_{E \times B}$  falls below  $-5\text{krad/s}$ .

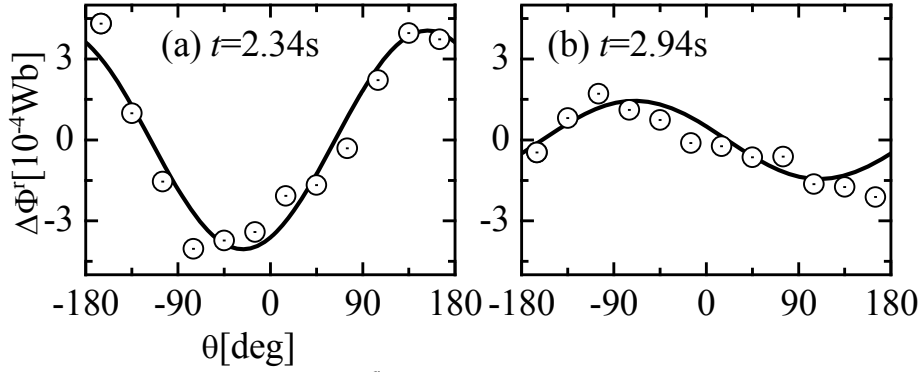


Fig.5 (LHD) Poloidal profile of  $\Delta\Phi^r$  for (a) island growing and (b) island healing.

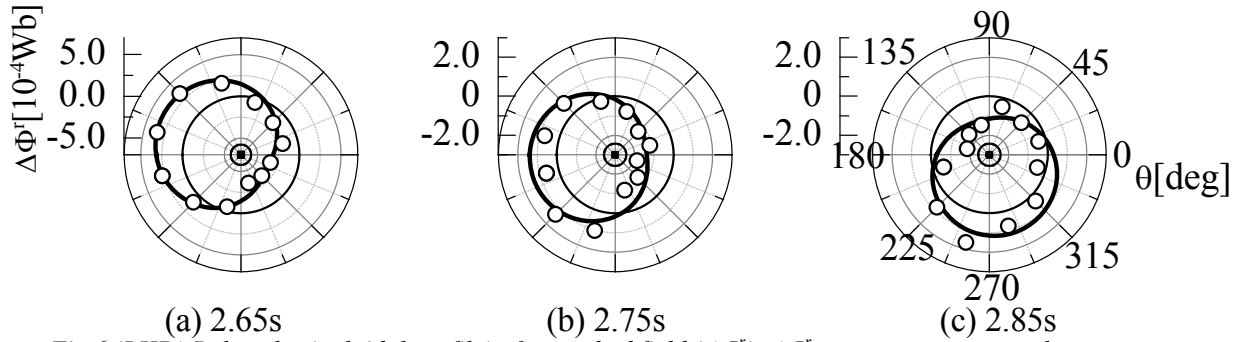


Fig.6 (LHD) Polar plot (poloidal profile) of perturbed field ( $\Delta\Phi^r$ ).  $\Delta\Phi^r$  structure rotates to electron-diamagnetic direction (counter clockwise).

amplitude of the sine wave with an  $m = 1$  component. The phase difference ( $\Delta\theta_{m=1}$ ) is defined as the difference between the poloidal angle of the X-point made by only  $\Delta\Phi^r$  and that of the seed island. The  $\Delta\Phi_{m=1}^r$  and  $\Delta\theta_{m=1}$  are  $\Delta\Phi_{m=1}^r = 4.1 \times 10^{-4} \text{Wb}$ ,  $\Delta\theta_{m=1} = -0.15\pi \text{rad}$  for a growing island and  $\Delta\Phi_{m=1}^r = 1.4 \times 10^{-4}$ ,  $\Delta\theta_{m=1} = -0.91\pi \text{rad}$  for a healing island. The toroidal mode,  $n$ , is determined as  $n = 1$  from a toroidal profile of the perturbed field measured by another flux-loop array [10]. The non-zero  $\Delta\Phi^r$  structure implies that a certain current with the same mode structure spontaneously flows in the plasma because we do not drive any current externally. That is to say, a current with  $m/n = 1/1$  mode flows in both cases (growing and healing), and their directions are opposite each other. Polar plots of  $\Delta\Phi^r$  during the transition are shown in Fig.6. The  $\Delta\Phi^r$  structure rotates to the electron-diamagnetic direction (counter clockwise). This result means that the structure of the current flowing in the plasma is modified by a poloidal flow and its direction is the same as the poloidal flow (electron-diamagnetic direction).

The time evolution of tangential-NB power, resonant field amplitude ( $\Delta\Phi_{m=1}^r/B_t$ ), difference of the poloidal angle of X-point from the seed island ( $\Delta\theta_{m=1}$ ), width of local flattening of  $T_e$  and  $\omega_{E \times B}$  at  $r_{\text{eff}} = 0.6 \text{m}$  are shown in Fig.7. The poloidal flow is measured from  $t = 2.34 \text{s}$  to  $2.94 \text{s}$  at intervals of  $0.1 \text{s}$ . The sequence of magnetic island dynamics is as follows: the  $|\omega_{E \times B}|$  (Fig.7(e)) increases from  $t = 2.34 \text{s}$  to  $2.54 \text{s}$  prior to the island being healed;  $\Delta\Phi_{m=1}^r/B_t$  starts decreasing at  $t = 2.62 \text{s}$  which means that the island width decreases (Fig.7 (b)). At that time, the  $|\omega_{E \times B}|$  further increases from  $6$  to  $13 \text{krad/s}$ . The  $\Delta\theta_{m=1}$  starts shifting (rotating) to the electron-diamagnetic direction at  $t = 2.67 \text{s}$  (Fig.7 (c)), which implies that the current sheet in the plasma is modified by the poloidal flow. Simultaneously, the width of local flattening of  $T_e$  decreases from  $\sim 0.1 \text{m}$  to  $0$  between  $t = 2.6$  and  $2.94 \text{s}$ . Finally, the magnetic island is healed.

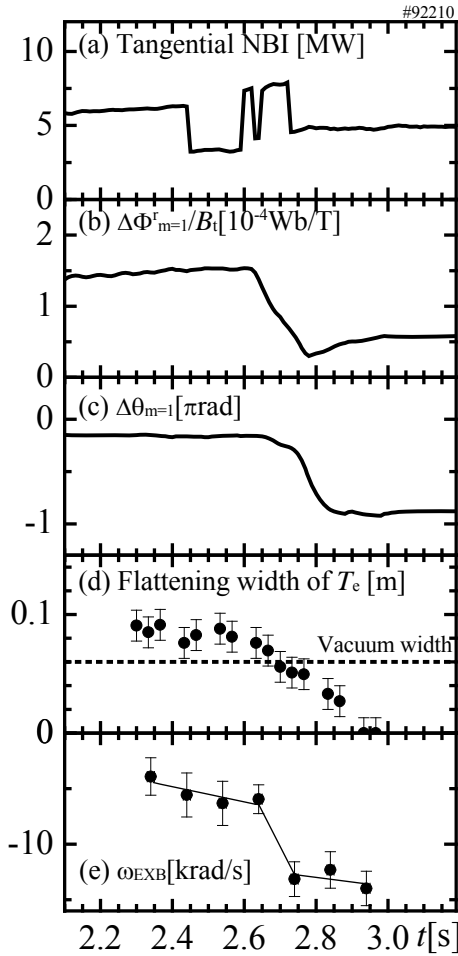


Fig.7 (LHD) Time evolution of (a) NBI, (b)  $\Delta\Phi_{m=1}^r/B_t$ , (c)  $\Delta\theta_{m=1}$ , (d) flattening width of  $T_e$  and (e)  $\omega_{E \times B}$ . Case of island transition from growth to healing.

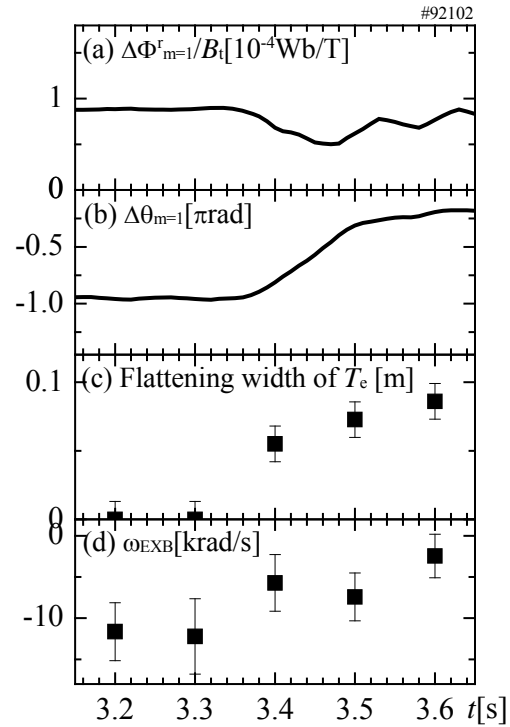


Fig.8 (LHD) Time evolution of (a)  $\Delta\Phi_{m=1}^r/B_t$ , (b)  $\Delta\theta_{m=1}$ , (c) flattening width of  $T_e$  and (d) poloidal flow in case of island transition from healing to growth.

### 2.3. Experimental Results in Transient State (healing to growth)

When the island transition is reversed (healing to growth), the poloidal flow decreases. Figure 8 shows waveforms of  $\Delta\Phi_{m=1}^r/B_t$ ,  $\Delta\theta_{m=1}$ , width of local flattening of  $T_e$  and  $\omega_{E \times B}$ . After the  $|\omega_{E \times B}|$  decreases between  $t = 3.3 - 3.4$ s, the width continues to grow to 0.1m until  $t = 3.6$ s and the  $\Delta\theta_{m=1}$  rotates to ion-diamagnetic direction between  $t = 3.36$  to 3.5s. These experimental results show the opposite trend to the case of transition from growing to healing.

## 3. Experiments in TJ-II

### 3.1. Experimental Setup of TJ-II

The TJ-II [14] is a Helic-type plasma confinement device. The TJ-II configuration consists of 32 toroidal field (TF) coils whose centres follow a toroidal helix of major radius 1.5 m, minor radius 0.28 m and pitch law  $\theta = -4\phi$  where  $\theta$  and  $\phi$  are the usual poloidal and toroidal angles, respectively. The magnetic configuration is completed by a central conductor made up of two coils: a pure horizontal circular one of 3 m diameter and a helical winding wrapped around the circular coil following the same winding law as the TF coils. There are two pairs of vertical field coils that control the radial position of the plasma, and two OH coils. It is possible to induce an Ohmic current in the plasma using these coils, which can modify the rotational transform ( $i/2\pi$ ) profile. The nominal magnetic field produced by these

coils at the centre of the plasma is 1T. The magnetic surfaces are bean-shaped for the entire operational space. Typical plasma major and averaged minor radii are  $R = 1.5$  and  $a = 0.22$  m, respectively.

### 3.2. Experimental Result in TJ-II

It is worthwhile to investigate the experimental facts in TJ-II [15] showing a similar behaviour of the island dynamics despite the different parameter range (mode number of island  $m/n = 2/4$ , lower magnetic shear, lower- $\beta$ , lower- $\nu$ , and ion-diamagnetic direction of  $\omega_{E \times B}$  etc.) from LHD.

Figure 9 shows the transition of the magnetic island from growth to healing. Before the transition, the local flattening region of SXR remarkably appears at  $\rho = -0.4$  to  $-0.2$  (Solid line in Fig.9). After the transition, it almost disappears and a small change of gradient remains which makes it difficult to judge whether the island exists or not (Dashed line in Fig.9). During the island healing, a strong positive radial electric field ( $E_r$ ) is thought to be established. In the TJ-II experiment, the positive  $E_r$  triggers the transition to the core electron-root confinement (CERC) plasma realized by means of the  $1/2\pi$  control by OH current in the ECH plasma, in which positive  $E_r$  is always observed [16] and increases at the same time as the jump of the  $T_e$  shown in Fig10 (a). As shown in Fig.10, island healing follows the CERC established at  $t = 1118$ ms. Before the CERC onset, the local flattening of soft X-ray profiles at  $\rho = 0.4$  appears at  $t = 1117$ ms as shown in Fig.9, which shows the existence of a magnetic island. The island lasts until  $t = 1120$ ms just after the CERC formation. After that, the magnetic island disappears at  $t > 1122$ ms. These experimental observations show that the  $\omega_{E \times B}$  changes prior to the island healing as seen in LHD.

### 4. Discussion

To explain the dynamics of the magnetic island, some kinds of effects have been considered. In the tokamak case, they have been summarized as the modified Rutherford equation [17], in which the bootstrap current and/or Pfirsch–Schlüter current and so on play key roles in the stability of the magnetic island. In the LHD experiment, bootstrap current and Pfirsch–Schlüter current could not explain the healing of the magnetic island [18].

In the TJ-II experiment, the increase of the

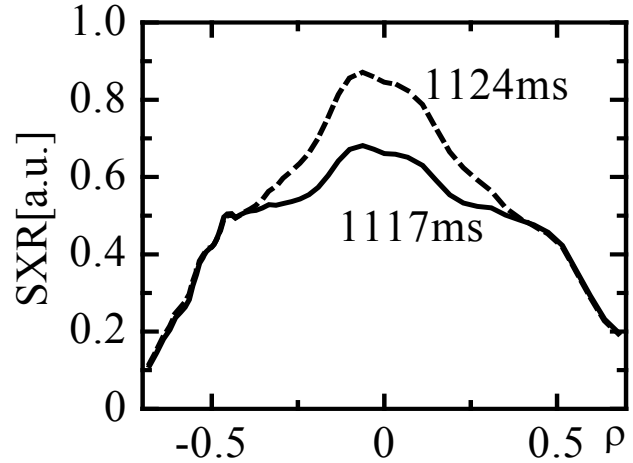


Fig.9 (TJ-II) Profile of SXR at  $t=1117$ ms (solid : before healing) and  $1124$ ms (dashed : after healing).

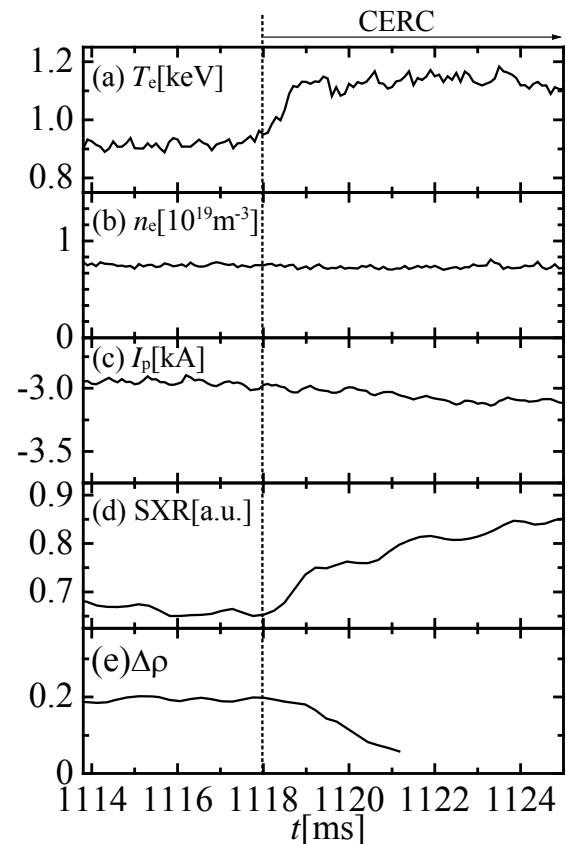


Fig.10 (TJ-II) Time evolution of (a) core electron temperature, (b) electron density, (c) plasma current, (d) SXR and (e) island width estimated from SXR profile.

radial electric field is important to trigger the CERC formation in which the magnetic island shows healing. Here, we pay attention to the correlation between poloidal flow and island dynamics. In the condition of the electron-root ( $E_r > 0$ ), the experimental observation of the CERC in TJ-II plasmas shows that the magnetic island is healed in the positive  $E \times B$  drift  $\omega_{E \times B} > 0$  (ion-diamagnetic direction). Furthermore, the CERC develops prior to the island healing. Namely, the poloidal flow with ion-diamagnetic direction increases prior to the island healing. In the LHD experiment, on the other hand, the radial electric field diagnosed by CXS is negative  $E_r < 0$ . The poloidal flow in the electron-diamagnetic direction outside the rational surface of  $\iota/2\pi = 1$  increases prior to the transition of the magnetic island from growth to healing, and vice versa. The rotation direction of the structure of current flowing in plasma is the same as the poloidal flow when the magnetic island transits from growth to healing. When the width of the magnetic island is comparable to the banana width, the ion polarization current effect on the stability should arise [19,20]. However, the above experimental observations show that the magnetic island could be stabilized in spite of its certain island width. Therefore, we have to take into account another mechanism. A candidate is the relationship between the viscous drag force and the magnetic torque. Due to the increase of the poloidal flow, the viscous drag force overcomes the magnetic torque between the externally imposed field and the current sheet. As a result, the current sheet is shifted (rotated) and the magnetic island is healed. From the above experiments, it is thought that the poloidal flow (radial electric field) is important to clarify the dynamics of the magnetic island, since it is a common feature of LHD and TJ-II.

## 5. Summary

In the LHD experiment, the poloidal flow in the electron-diamagnetic direction outside the rational surface increases prior to the transition of the magnetic island from growth to healing whereas the poloidal flow in the ion-diamagnetic direction at the rational surface increases in TJ-II. The temporal increment of the poloidal flow is followed by the transition (growth to healing) of the magnetic island regardless of the flow direction. These experimental observations from LHD and TJ-II clarify the fact that a significant poloidal flow affects the magnetic island dynamics. It is thought that due to the increase of the poloidal flow, the viscous drag force overcomes the magnetic torque between the externally imposed field and the current sheet. As a result, the current sheet is shifted (rotated) and heals the magnetic island.

## Acknowledgements

The authors are grateful to the LHD operation group and TJ-II operation group for their excellent technical support. One of authors (N.Y.) also thanks to the administration department in NIFS for their tireless dedication. This work was supported by a Grant-in-Aid for Young Scientists (B) (No. 22760661) from the Ministry of Education, Culture, Sports, Science and Technology of Japan. This work is also supported by the budget NIFS10ULPP014 of the National Institute for Fusion Science.

## References

- 
- [1] WAELBROECK, F. L., Nuclear Fusion **49** (2009) 104025
  - [2] FENG, Y., SARDEI, F., GRIGULL, et al., Nuclear Fusion **46** (2006) 807
  - [3] CASTEJÓN, F., FUJISAWA, A., et al., Plasma Phys. Control. Fusion **47** (2005) B53
  - [4] IDA, K., INAGAKI, S., TAMURA, N., et al., Nucl. Fusion **44** (2004) 290
  - [5] INAGAKI, S., IDA, K., et al., Plasma Phys. Control. Fusion **46** (2004) A71
  - [6] LÓPEZ-BRUNA, D., ESTRADA, T., et al., Europhysics Letter **82** (2008) 65002

- 
- [7] ASCASÍBAR, E., LÓPEZ-BRUNA, D., et al., Plasma Fusion Res. **3** (2008) S1004
  - [8] CASTEJÓN, F., LÓPEZ-BRUNA, D., ESTRADA, T., et al., Nucl. Fusion **44** (2004) 593
  - [9] MORISAKI, T., OHYABU, N., et al., Phys. of Plasmas **14** (2007) 056113
  - [10] MORISAKI, T., MASUZAKI, S., SUZUKI, H., et al., Fusion Eng. Des. **65** (2003) 475
  - [11] IDA, K., KADO, S., and LIANG, Y., Rev. Sci. Instruments **71** (2000) 2360
  - [12] NARUSHIMA, Y., WATANABE, K.Y., et al., Plasma Fusion Res. **2** (2007) S1094
  - [13] NARUSHIMA, Y., WATANABE, K.Y., SAKAKIBARA, S., et al., Nucl. Fusion **48** (2008) 075010
  - [14] ALEJALDRE, C., et al., Fusion Technol. **17** (1990) 131
  - [15] ESTRADA, T., MEDINA, F., LÓPEZ-BRUNA, D., et al., Nucl. Fusion **47** (2007) 305
  - [16] ESTRADA, T., KRUPNIK, L., et al., Plasma Phys. Control. Fusion **46** (2004) 277
  - [17] MIKHAILOVSKII, A.B., Contrib. Plasma Phys. **43** (2003) 125
  - [18] NARUSHIMA, Y., WATANABE, K.Y., et al., Fusion Sci. Technol. **58** (2010) 194
  - [19] T. OZEKI, et al., " Effects of Plasma Rotation on the Neoclassical Tearing Mode in JT-60U" Proc. 28th EPS (Madeira 2001) ECA **25A**, P-4.003, 1345
  - [20] V.D. PUSTOVITOV, et al., " Theory of Neoclassical Tearing Modes and its Application to ITER" 18th IAEA Fusion Energy Conference (2000), IAEA-CN-77/ITERP/07